Eur Radiol (2006) 16: 1367–1373
DOI 10.1007/s00330-005-0128-7

Setsuko Kawase
Shinji Naganawa
Michihiko Sone
Mitsuru Ikeda
Takeo Ishigaki

Relationship between CT densitometry with a slice thickness of 0.5 mm and audiometry in otosclerosis

Received: 13 July 2005
Revised: 9 October 2005
Accepted: 13 December 2005
Published online: 11 March 2006

S. Kawase (✉) · S. Naganawa · T. Ishigaki
Department of Radiology, Nagoya University Graduate School of Medicine, 65 Tsurumai-cho, Shouwa-ku, Nagoya, 466-8550, Japan
e-mail: secy@nifty.com
Tel.: +81-52-7442327
Fax: +81-52-7442335

M. Sone
Department of Otorhinolaryngology, Nagoya University Graduate School of Medicine, 65 Tsurumai-cho, Shouwa-ku, Nagoya, 466-8550, Japan

M. Ikeda
Department of Radiological Technology, Nagoya University School of Health Sciences, 1-1-20 Taikou-minani, Higashi-ku, Nagoya, 461-8673, Japan

Abstract The appropriate cutoff Hounsfield unit (HU) value for the diagnosis of otosclerosis was determined and the correlation between the bone conduction threshold and the findings of computed tomography (CT) densitometry investigated. CT images, 0.5-mm thick, were evaluated in 24 ears with otosclerosis and 19 control ears. Eight regions of interest were set around the otic capsule. The mean HU values in the area anterior to the oval window (A-OW) and anterior to the internal auditory canal (A-IAC) were significantly lower in otosclerosis than in controls. Based on receiver operating characteristic (ROC) analysis, the cutoff HU value in A-OW was determined to be 2,187.3 HU. The mean HU value in retrofenestral otosclerosis was significantly lower in the area A-OW, A-IAC and around the cochlea than in controls. Based on ROC analysis, the cutoff HU value in the latter was determined to be 2,045 HU. A statistically significant correlation was found between the density of the area A-OW and the hearing level at 500 and 1,000 Hz, and between the density of the area around the cochlea and the hearing level at most frequencies. These results suggest the semi-automated diagnosis of otosclerosis may be possible.

Keywords Otosclerosis · Densitometry · Computed tomography · Audiometry

Introduction

Otosclerosis is an osseous remodeling disorder limited to the otic capsule of the temporal bone [1, 2]. The lesion in otosclerosis is pleomorphic; i.e., the lesion is initially spongiotic and is then replaced by fibrous tissue and becomes sclerotic [1, 2]. It is said that the earliest changes occur in the otic capsule anterior to the oval window and that the lesion then spreads around the cochlea and vestibule [1, 2].

Otosclerosis is diagnosed based on the patient's clinical history, physical findings, audiometric testing, and radiological examinations [3–11]. Computed tomography (CT) and magnetic resonance imaging (MRI) have been reported to be useful for the diagnosis of otosclerosis [4–13]. The active lesion in otosclerosis is shown as an enhancing

lesion in contrast-enhanced MR images [7, 12, 13]. However, the modality of choice for the imaging evaluation of otosclerosis is generally CT [14]. CT images play an important role in assessing the extent of the lesion in otosclerosis and the severity of destructive and sclerotic foci [4, 9, 15]. CT images show overgrowth of abnormally hypoattenuating bone in the region of the fissula ante fenestram in the fenestral type and show a hypoattenuating halo around the cochlea in the retrofenestral type [3, 4].

Although the CT densitometry of fenestral otosclerosis and the correlation between CT densitometry and audiometry have been reported [16–22], there have been few reports concerning CT densitometry or the cutoff value for the diagnosis of otosclerosis using CT images with a slice thickness of 0.5 mm.

The purpose of the present study was to determine the appropriate cutoff Hounsfield unit (HU) value for the diagnosis of otosclerosis and to investigate the correlation between the bone conduction threshold and the findings of CT densitometry.

Materials and methods

Patients and controls

This study was performed in consecutive patients in the period from May 2000 to November 2002. Twenty-four ears of 17 patients with otosclerosis (seven females and ten males) and 19 normal ears of 19 patients (ten females and nine males) were evaluated. The control ears were the opposite normal ears in patients with otitis media, cholesteatoma, trauma, surgical trauma, or tinnitus. They showed normal CT and audiometry findings and were diagnosed as normal by an otorhinolaryngologist and radiologists. The final diagnosis of otosclerosis is the basis of clinical history, physical findings, audiometric test and CT imaging. CT imaging is used for rule out other possible conductive hearing loss. The patients ranged in age from 6 to 77 years (mean, 41.96±21.7 years) in the otosclerosis group and from 7 to 72 years (mean, 43.63±21.56 years) in the control group (Table 1). When otosclerosis was suspected by the otorhinolaryngologist, CT examination was performed. The diagnosis of otosclerosis based on CT images was prospectively established by the consensus of two neuroradiologists in our department. The diagnostic criterion for fenestral otosclerosis was the overgrowth of abnormally hypoattenuating bone in the fissula ante fenestram and the criterion for retrofenestral otosclerosis was the presence of a hypoattenuating halo around the cochlea [4] (Fig. 1). The diagnosis was surgically confirmed in three of these 24 ears.

Table 1 Summary of the subjects

	Controls	Otosclerosis
Age	43.63(±21.6)	41.96(±21.7)
Number of Subjects	19	17
Sex		
Male	9	10
Female	10	7
Number of ears	19	24
CHL	0	6
SNHL	0	5
MHL	0	13

( ): ±standard deviation
CHL: conductive hearing loss; SNHL: sensorineural loss; MHL: mixed hearing loss

CT examination

All CT images were obtained using a four-detector-row CT scanner (Aquilion, Toshiba Medical Systems Corporation, Tokyo, Japan) with 0.5-mm collimation and a 512×512 matrix. Scan conditions were 140 kV, 300 mAs, and 1 s/rotation in non-helical mode. In the axial slice depicting the footplate of the stapes and the modiolus, eight circular regions of interest (ROIs) were manually set by the radiologist. HU value at each ROI was obtained from a single measurement. Details of ROI setting are shown in Table 2.

Fig. 1 A 24-year-old man with otosclerosis (fenestral and retrofenestral lesions). An area of hypodensity anterior to the oval window is depicted in a CT image with 0.5-mm collimation (fenestral lesion, *white arrow*). Demineralization of the otic capsule, with a hypodense defect outlining the cochlea, is seen as the retrofenestral lesion (*black arrow*)

Table 2 The ROI setting

ROI #1:	the area of 1 mm posterior to the oval window
ROI #2:	the area of 1 mm anterior to the oval window
ROI #3:	the area of 1 mm lateral to the interscalar septum between basal and middle turn of the cochlea
ROI #4:	the area of 1 mm anterolateral to the apex of the cochlea
ROI #5:	the area of 1 mm anterior to the apex of the cochlea
ROI #6:	the area of 1 mm anteriomedial to the interscalar septum between basal and middle turn of the cochlea
ROI #7:	the area of 1 mm anteromedial to basal turn of the cochlea
ROI #8:	the area of 1 mm anterior to wall of the internal auditory canal

The area of each ROI was 1 mm^2, and the mean HU value in each ROI was measured. An example of ROI setting is shown in Fig. 2. One otosclerotic lesion was directly visible on CT images in 18 ears of the 24 ears and more otosclerotic foci were visible in six ears.

Audiometric testing

Audiometric tests were performed in a double-walled sound room within 2 months before or after CT examination. Testing was not performed in one patient in the normal group. Air conduction, bone conduction, and the air-bone gap threshold were recorded at 250, 500, 1,000, 2,000, 4,000, and 8,000 Hz. The hearing levels for air conduction and bone conduction were calculated using the formula (500 Hz + 2×1,000 Hz + 2×2,000 Hz + 4,000 Hz)/6. Conductive hearing loss (CHL) was diagnosed if the air-bone gap was more than 15 dB and bone conduction was less than 30 dB. Sensorineural hearing loss (SNHL) was diagnosed when the air-bone gap was less than 15 dB and bone conduction was more than 30 dB. Mixed hearing loss (MHL) was diagnosed when the air-bone gap was more than 15 dB and bone conduction was more than 30 dB. Six of the 24 ears with otosclerosis showed CHL, five ears showed SNHL, and 13 ears showed MHL.

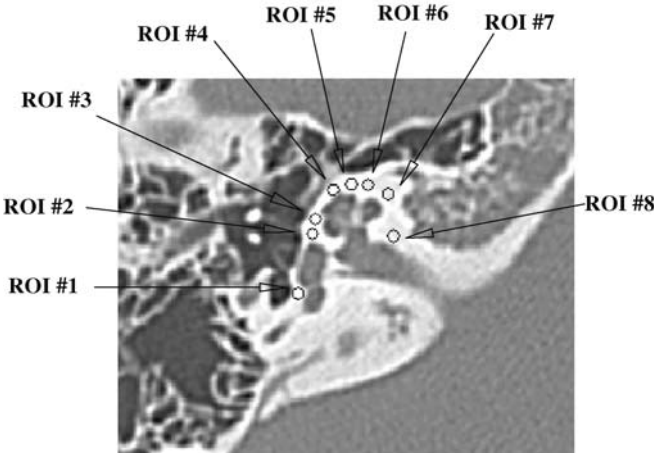

Fig. 2 Example of ROI setting. In the axial slice including the foot plate and modiolus, eight ROIs are manually placed. Each ROI has an area of 1 mm^2

Data analysis

CT densitometry results for each ROI (from ROI 1 to ROI 8) were evaluated using the Student's *t*-test to compare the 24 ears with otosclerosis against the 19 normal ears (first analysis pattern). To determine the appropriate cutoff HU value for the diagnosis of otosclerosis, receiver operating characteristic (ROC) analysis was performed. For ROC analysis, a binormal ROC curve was fitted to each mean HU value in a given ROI using a maximum-likelihood estimation. The area under the binormal ROC curve was used as an index of diagnostic performance.

Here, to focus on retrofenestral otosclerosis, the 18 ears with otosclerosis that showed SNHL or MHL were also compared against the 19 normal ears (second analysis pattern).

Furthermore, in order to evaluate the linear relationship between CT densitometry findings and hearing loss at specific frequencies, the pairwise Pearson correlation coefficients between the mean CT value in each ROI and bone conduction at each frequency were calculated in the normal ears and in all ears with otosclerosis (24 ears).

In the statistical analysis, a value of $P<0.05$ was accepted as significant.

Results

In the first analysis pattern, the mean HU value of the ears with otosclerosis was significantly lower in ROI 2 (i.e., the area 1 mm anterior to the oval window) and ROI 8 (i.e., the area of 1 mm anterior to wall of the internal auditory canal) compared with the normal ears, as shown in Table 3 and Fig. 3 (ROI 2, $P<0.001$; ROI 8, $P=0.0285$). No significant differences were observed between the ears with otosclerosis and the normal ears in the other ROIs.

Figure 4 shows the binormal ROC curve for CT densitometry of ROI 2, because it is thought ROI 2 is more significant difference than ROI 8. The area under the binormal ROC curve (A_z) was 0.92. The threshold CT value for the point on this ROC curve at which sensitivity and specificity were equal was 2,187.3 HU, and the sensitivity (specificity) at that point was 85.21% (Fig. 4).

In the second analysis pattern, when the ears with otosclerosis were restricted to the 18 ears with SNHL or

Table 3 The mean HU value of ROIs

ROI	Controls	Otosclerosis	Otosclerosis with SNHL and MHL
1	2280.96±356.96	2222.02±345.48	2190.13±286.15
2	2416.44±211.87	1382.89±764.06	1285.35±780.78
3	2386.50±244.83	2218.40±312.44	2217.71±321.95
4	2352.95±309.35	2199.28±343.87	2197.42±380.29
5	2179.57±202.37	1970.45±509.95	1920.14±579.65
6	2111.29±121.27	1961.82±306.62	1932.10±341.86
7	2014.44±86.53	1937.03±386.02	1893.93±439.17
8	1971.27±139.43	1634.56±613.16	1638.07±618.22

Values are expressed as means ± standard deviation

MHL, the mean ROI value of the ears with otosclerosis was significantly lower in ROI 2, ROI 6 (i.e., the area 1 mm anteromedial to the interscalar septum between the basal and middle turns of the cochlea) and ROI 8 compared with the normal ears, as shown in Table 3 and Fig. 5 (ROI 2, $P<0.001$; ROI 6, $P=0.0387$; ROI 8, $P=0.0327$). No significant differences were detected between the ears with otosclerosis and the normal ears in the other ROIs.

Considering only the 18 ears with SNHL or MHL, the binormal ROC curve for ROI 6 is shown in Fig. 6. The A_z value was 0.72. The threshold CT value for the point on this ROC curve at which sensitivity and specificity were equal was 2,045 HU, and the sensitivity (specificity) was 68.11% (Fig. 6).

Secondly, the linear relationships between the CT densitometry and hearing loss were evaluated at specific frequencies. Statistically significant correlations were found between the CT density in ROI 2 and the hearing level at 500 Hz ($P=0.0213$) and 1,000 Hz ($P=0.0296$). There were also significant correlations between ROI 5 (i.e., the area 1 mm anterior to the apex of the cochlea) and the hearing level at 250 Hz ($P=0.002$), 500 Hz ($P<0.001$), 1,000 Hz ($P<0.001$), 2,000 Hz ($P=0.004$), and 4,000 Hz ($P=0.0273$). In ROI 6 (i.e., the area 1 mm anteromedial to the interscalar septum between the basal and middle turns of the cochlea), there were significant correlations at all frequencies (250 Hz, $P<0.001$; 500 Hz, $P<0.001$; 1,000 Hz, $P<0.001$; 2,000 Hz, $P=0.0027$; 4,000 Hz, $P=0.0234$; and 8,000 Hz, $P=0.0475$) (Fig. 7).

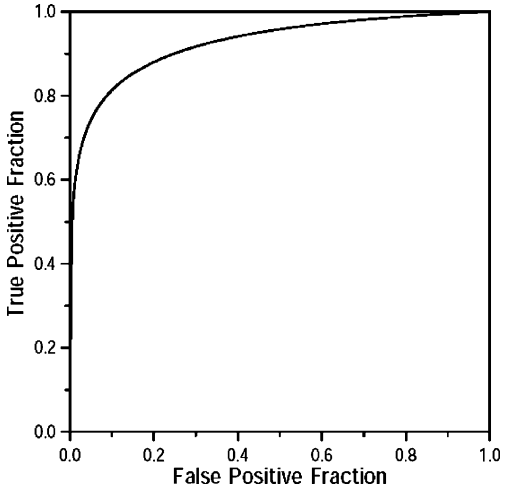

Fig. 4 ROC curve of ROI 2 in otosclerosis. The area under the binormal ROC curve (Az): 0.9262; negative diagonal: 2,187.3 HU

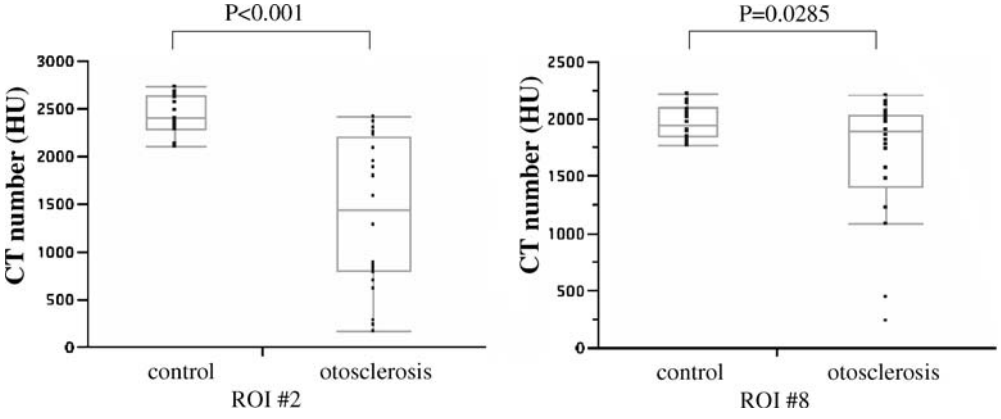

Fig. 3 Mean values of average density in ROI #2 and ROI #8 HU: Hounsfield unit, ROI: region of interests, ROI #2: the area anterior to the oval window, ROI #8: the area anterior to the wall of the internal auditory canal A statistically significant difference was found between the control and otosclerosis groups in ROI #2 (Student's t-test, p<0.001) and ROI #8 (Student's t-test, p=0.0285). Box-whisker plots of CT number (HU) values are shown. The center horizontal line indicates the median value. The bottom and top edges of the box indicate the 25th and 75th percentiles.

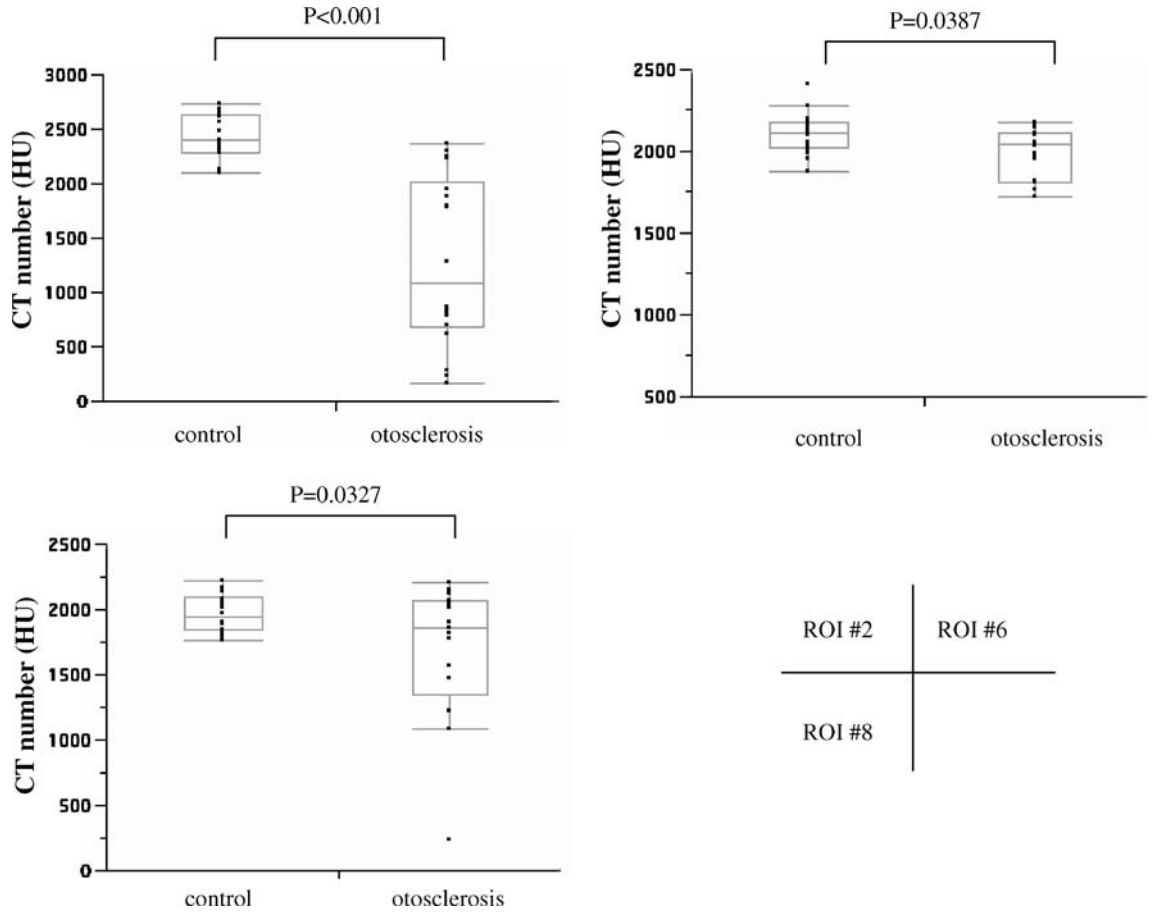

Fig. 5 Mean values of average density in ROIs 2, 6 and 8 in controls and patients with otosclerosis with MHL and SNHL. Statistically significant differences between the control and otosclerosis groups were found in ROI 2 (Student's *t*-test, $P<0.001$), ROI 6 (Student's *t*-test, $P=0.0387$) and ROI 8 (Student's *t*-test, $P=0.0327$). Box-whisker plots of CT number (HU) values are shown. The center *horizontal line* indicates the median value. The *bottom and top edges* of the box indicate the 25th and 75th percentiles. The *vertical line* indicates the range of data

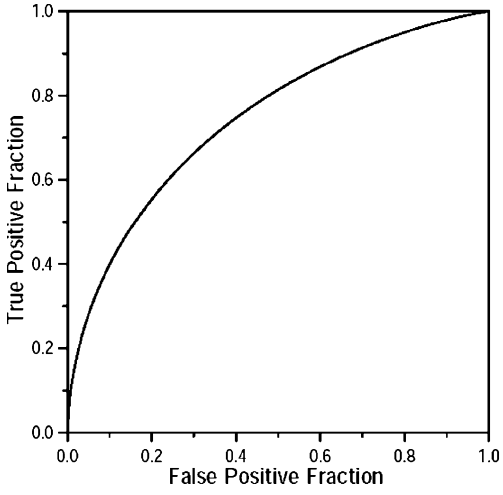

Fig. 6 ROC curve of ROI 6 in otosclerosis with SNHL. The area under the binormal ROC curve (Az): 0.7469; negative diagonal: 2,045 HU

Discussion

Structural details can be clearly visualized by CT when thin slices, such as a slice thickness of 0.5 mm, are used. This is due to the elimination of partial volume effects [23]. This is considered to be particularly useful for the evaluation of extremely small anatomical structures such as those in the temporal bone [24, 25].

Analysis of CT densitometry findings with a slice thickness of 0.5 mm was performed using two analysis patterns. In the first analysis pattern, the mean HU values of the ears with otosclerosis were compared with the normal ears. In the second analysis pattern, the mean HU values of the ears with otosclerosis and SNHL or MHL were compared with the normal ears. The second analysis pattern was assumed to correspond to retrofenestral otosclerosis. In retrofenestral otosclerosis, CT is used for the more sensitive imaging evaluation of the otic capsule [8, 26].

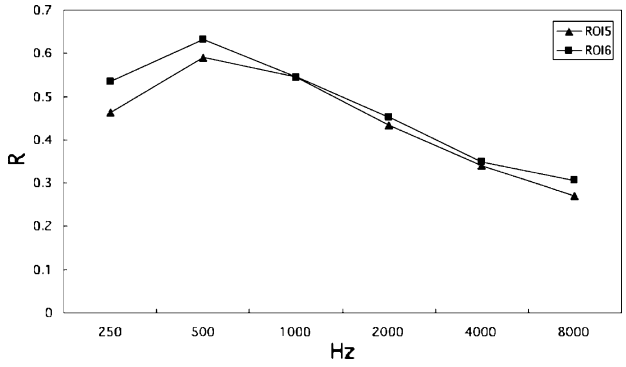

Fig. 7 Correlation coefficients in ROI 5 and ROI 6 in otosclerosis. The correlation coefficient (*R*) was highest at 500 Hz for both ROI 5 and 6

In addition, an attempt was made to determine the appropriate cutoff value for the diagnosis of otosclerosis from these analyses. Areas of radiolucency may be seen to be mixed with sclerotic changes in otosclerosis [6]. Because it may not be possible to diagnose this remineralized phase using CT [19], the macroscopic diagnosis of otosclerosis is sometimes difficult. Therefore, we attempted to determine the appropriate cutoff HU value by ROC analysis.

In the first analysis pattern, a significant difference was found in ROI 2 (i.e., the area 1 mm anterior to the oval window) and ROI 8 (i.e., the area of 1 mm anterior to wall of the internal auditory canal). Huizing and de Groot [17] performed CT densitometry of the capsule of the cochlea with a slice thickness of 1.5 mm, although they were not able to establish a site of predilection for otosclerotic foci. In a study involving CT densitometry of the capsule of the cochlea with a slice thickness of 1 mm, Miura et al. [16] confirmed that the mean value in the area anterior to the oval window was significantly lower in fenestral otosclerosis, as was found in our study. Grayeli et al. [22] showed bone density in the fissula ante fenestram (corresponding to ROI 2) and posterior semicircular canal (the area near ROI 1) were lower in otosclerosis groups with a slice thickness of 0.5 mm [22]. There was no significantly difference in anterior margin of the internal auditory canal (corresponding to ROI 8) between controls and otosclerosis. The cutoff HU value in that area was not determined in the previous study. The cutoff HU value in ROI 2 was found to be 2,187 HU by ROC analysis. The area under the binormal ROC curve (Az) was 0.92, and it is suggested that this value may be useful in the radiological diagnosis of otosclerosis in combination with other diagnostic methods.

In the second analysis pattern, ROI 2, ROI 6 (i.e., the area 1 mm anteromedial to the interscalar septum between the basal and middle turns of the cochlea) and ROI 8 showed significant differences compared with controls. From the second analysis pattern, we attempted to determine the appropriate cutoff HU value for the diagnosis of retrofenestral otosclerosis. Most ears with retrofenestral otosclerosis show involvement not only of the cochlea (corresponding to ROI 6) but also the fissula ante fenestram (corresponding to ROI 2) [4, 14]. In this study, ROI 6 was selected as the area for determining the cutoff HU value for retrofenestral otosclerosis because ROI 2 was selected as the area for determining the cutoff HU value for fenestral otosclerosis (the first analysis pattern in the present study). The cutoff HU value was determined to be 2,045 HU based on ROC analysis. The area under the binormal ROC curve (A_z) was 0.75, and it was judged that the diagnostic performance of CT densitometry is acceptable for retrofenestral otosclerosis.

In CT images of the temporal bone, the normally hypoattenuating area called the cochlear cleft was seen in the otic capsule lateral to the middle turn of the cochlea [29]. The incidence of the cochlear cleft has been reported to be 62% in the youngest group (less than 4 years of age), falling to 19% in the oldest groups (teenagers) [29]. In the present study, the mean ages were 41 years in the control groups and 43 years in the otosclerosis groups. Furthermore, the cochlear cleft corresponded to ROI 3 in the present study, and there were no differences between the control and otosclerosis groups in densitometry. Therefore, it is concluded that there is no need to consider the cochlear cleft in interpreting the findings of this study.

Negative correlations between the mean CT value in each ROI and the bone conduction threshold were found in ROI 2, ROI 5 (i.e., the area 1 mm anterior to the apex of the cochlea), and ROI 6. In particular, the CT values in ROIs 5 and 6 showed the highest correlation at 500 Hz, as shown in Fig. 7.

High tones show maximal vibration near the basilar turn, medium tones in the middle turns, and low tones in the apical turn [27]. The highest audible frequency of approximately 20,000 Hz is associated with the membrane behind the round window, and the apical end corresponds to a frequency of just 60 Hz [27]. Swartz et al. [19] have shown a correlation between decalcification of the otic capsule and SNHL at high, middle, and low frequencies, although quantitative evaluation, such as densitometry, was not performed. In other reports using a 1.5-mm slice thickness, it has been shown that the highest correlation is seen in the middle cochlear turn or the basal cochlear turn [18, 19]. In the present study, although the highest negative correlation was observed in ROIs 2, 5, and 6, corresponding to the middle turn, no clear correlations were found between the position of decalcification and the hearing loss frequency. It is thought that the cause of the hearing loss, i.e., a reduction in cochlear blood flow or the condition known as hyalinization by enzymes [1, 28], may not be detectable by CT.

In the present study, CT images were found to be useful for visualizing decalcification, but sclerotic changes were not detectable. Furthermore, surgical or autopsy confirmation was not performed in most of our cases. Further studies

including pathological evaluation are needed to confirm these findings.

Acknowledgement The authors are grateful to T. Kawase for valuable discussions and suggestions.

References

1. Linthicum FH Jr (1993) Histopathology of otosclerosis. Otolaryngol Clin North Am 26:335–352
2. Davis GL (1987) Pathology of otosclerosis: a review. Am J Otolaryngol 8:273–281
3. Lemmerling M (2004) Otosclerosis. In: Kollias SS (ed) Radiology of the petrous bone. Springer, Berlin Heidelberg New York (Tokyo), pp 91–98
4. Weissman JL (1996) Hearing loss. Radiology 199:593–611
5. Sakai O, Curtin HD, Fujita A, Kakoi H, Kitamura K (2000) Otosclerosis: computed tomography and magnetic resonance findings. Am J Otolaryngol 21:116–118
6. Vartiainen E, Saari T (1993) Value of computed tomography (CT) in the diagnosis of cochlear otosclerosis. Clin Otolaryngol 18:462–464
7. Stimmer H, Arnold W, Schwaiger M, Laubenbacher C (2002) Magnetic resonance imaging and high-resolution computed tomography in the otospongiotic phase of otosclerosis. ORL J Otorhinolaryngol Relat Spec 64:451–453
8. Mafee MF, Henrikson GC, Deitch RL et al (1985) Use of CT in stapedial otosclerosis. Radiology 156:709–714
9. Valvassori GE (1993) Imaging of otosclerosis. Otolaryngol Clin North Am 26:359–371
10. Blakley BW, Hilger PA, Taylor S, Hilger J (1986) Computed tomography in the diagnosis of cochlear otosclerosis. Otolaryngol Head Neck Surg 94:434–438
11. Barr MS, Lewin JS (1993) Computed tomographic evaluation of otosclerosis. Am J Otolaryngol 14:282–284
12. Ziyeh S, Berger R, Reisner K (2000) MRI-visible pericochlear lesions in osteogenesis imperfecta type I. Eur Radiol 10:1675–1677
13. Huber AM, Ma F, Felix H, Linder T (2003) Stapes prosthesis attachment: the effect of crimping on sound transfer in otosclerosis surgery. Laryngoscope 113:853–858
14. Swartz JD, Harnsberger HR (1998) Imaging of the temporal bone, 3rd edn. Thieme, New York
15. Veillon F, Riehm S, Emachescu B et al (2001) Imaging of the windows of the temporal bone. Semin Ultrasound CT MR 22:271–280
16. Miura M, Naito Y, Takahashi H, Honjo I (1996) Computed tomographic image analysis of ears with otosclerosis. ORL J Otorhinolaryngol Relat Spec 58:200–203
17. Huizing EH, de Groot JA (1987) Densitometry of the cochlear capsule and correlation between bone density loss and bone conduction hearing loss in otosclerosis. Acta Otolaryngol 103:464–468
18. Guneri EA, Ada E, Ceryan K, Guneri A (1996) High-resolution computed tomographic evaluation of the cochlear capsule in otosclerosis: relationship between densitometry and sensorineural hearing loss. Ann Otol Rhinol Laryngol 105:659–664
19. Swartz JD, Mandell DW, Berman SE, Wolfson RJ, Marlowe FI, Popky GL (1985) Cochlear otosclerosis (otospongiosis): CT analysis with audiometric correlation. Radiology 155:147–150
20. Hu H (1999) Multi-slice helical CT: scan and reconstruction. Med Phys 26:5–18
21. Kiyomizu K, Tono T, Yang D, Haruta A, Kodama T, Komune S (2004) Correlation of CT analysis and audiometry in Japanese otosclerosis. Auris Nasus Larynx 31:125–129
22. Grayeli AB, Yrieix CS, Imauchi Y, Cyna-Gorse F, Ferrary E, Sterkers O (2004) Temporal bone density measurements using CT in otosclerosis. Acta Otolaryngol 124:1136–1140
23. Katada K (2001) Usefulness of isotropic volumetric data in neuroradiological diagnosis. In: Reiser MF et al (eds) Multislice CT. Springer, Berlin Hedelberg New York, pp 109–117
24. Krombach GA, Schmitz-Rode T, Prescher A, DiMartino E, Weidner J, Gunther RW (2002) The petromastoid canal on computed tomography. Eur Radiol 12:2770–2775
25. d' Archambeau O, Parizel PM, Koekelkoren E, Van De Heyning P, De Schepper AM (1990) CT diagnosis and differential diagnosis of otodystrophic lesions of the temporal bone. European Journal of Radiology 11:22–30
26. Youssef O, Rosen A, Chandrasekhar S, Lee HJ (1998) Cochlear otosclerosis: the current understanding. Ann Otol Rhinol Laryngol 107:1076–1079
27. Stanley AG (2001), Essentials of audilogy, 2nd edn. Thieme, New York
28. Nakashima T, Naganawa S, Sone M, Tominaga M, Hayashi H, Yamamoto H, Liu X, Nuttall AL (2003) Disorders of cochlear blood flow. Brain Res Brain Res Rev 43:17–28
29. Chadwell JB, Halsted MJ, Choo DI, Greinwald JH, Benton C (2004) The cochlear cleft. Am J Neuroradiol 25:21–24